Modeling of Carbon Dioxide (CO$_2$) – Natural Gas Separation Using Membrane

by

Amy Goh Hui Ping (9751)

Dissertation submitted in partial fulfillment of

the requirements for the

Bachelor of Engineering (Hons)

Chemical Engineering

MAY 2011

Universiti Teknologi PETRONAS

Bandar Seri Iskandar

31750 Tronoh

Perak Darul Ridzuan

CERTIFICATION OF APPROVAL

Modeling of Carbon Dioxide (CO_2) – Natural Gas Separation Using Membrane

by

Amy Goh Hui Ping

A project dissertation submitted to the

Chemical Engineering Programme

Universiti Teknologi PETRONAS

in partial fulfillment of the requirement for the

BACHELOR OF ENGINEERING (Hons)

(CHEMICAL ENGINEERING)

Approved by,

_____

(Dr. Lau Kok Keong)

Project Supervisor

UNIVERSITI TEKNOLOGI PETRONAS

TRONOH, PERAK

May 2011

i

CERTIFICATION OF ORIGINALITY

This is to certify that I am responsible for the work submitted in this project, that the original work is my own except as specified in the references and acknowledgements, and that the original work contained herein have not been undertaken or done by unspecified sources or persons.

AMY GOH HUI PING

ABSTRACT

Currently, the existing methodology for carbon dioxide (CO_2) removal is not sufficient to remove high concentration of CO_2 in our natural gas supply. At the moment, the use of membrane separators is gaining popularity as years passed by and is slowly replacing absorption system to remove high CO_2 content. By using membrane gas separation units, they are smaller than other types of plants as compared to amine stripping plants. Therefore, have relatively small footprints as it is important in environments such as offshore gas-processing platforms.

In this study, 6FDA-TADPO polypyrrolone, which is a dense polymeric organic membrane model, will be analyzed. By collaborating dual-mode sorption model together with bulk flux contribution, the study of selectivity and permeability of carbon dioxide and methane in natural gas towards the membrane is done using Matrix Laboratory (MATLAB) where the behavior of the gases at certain pressure and composition is determined. The results obtained from the model are then validated with experimental data.

ACKNOWLEDGEMENT

I would like to take this opportunity to acknowledge all parties who put in most effort in making this Final Year Project successful and memorable. It is indeed a golden opportunity for me to learn and apply engineering skills in this project.

First and foremost, I would like to express my deepest gratitude to the coordinator of Final Year Project from the Chemical Engineering Department, namely Dr. Mohanad M.A.A El-Harbawi for his dedication and efforts in guiding me into better understanding about this research-based course.

I would also like to express my utmost and sincere appreciation and gratitude to my supervisor, Dr. Lau Kok Keong for his guidance, advices, assistance and support throughout the project. He had suggested me to take on this project and has since been very kind to help in various ways.

Also to my mentor, Ms. Wahyu, who sincerely assisted me in this project and guiding me all the time. Her attentiveness and advices were very well received and helpful to me.

Last but not least, many thanks to my family members and fellow friends for their continuous moral and emotional support to motivate me to pursue greater heights in this project.

TABLE OF CONTENTS

LIST OF FIGURES

LIST OF TABLES

LIST OF ABBREVIATIONS

CO_2	Carbon dioxide
CH_4	Methane
O_2	Oxygen
H_2S	Hydrogen Sulphide
MATLAB	Matrix Laboratory

CHAPTER 1

INTRODUCTION

1.1   Background of Study

Natural gas is an energy source can be used both at home (for cooking, heating) and in the industry. The production of certain liquid fuels uses natural gas as a raw material. Natural gas is also used for the production of electricity, pulp and paper, metals, chemicals, stone, clay, glass, and to process certain foods or treat waste materials (Abou-Arab, 1986).

As the demand for natural gas continues to increase, new or previously ignored areas of gas supplies are being revisited. Many of these new gas supplies have been ignored in the past due to poor gas quality or prohibitive costs associated with treating the gas to make it saleable. However, as gas prices have continued to rise and new gas treating technologies have been developed, the prospect of treating and selling these gas volumes has become viable.

These new gas sources include coal bed seam gas, landfill gas and bio-digester gas, to name a few. Each of these gas streams can contain up to 50% to 80% carbon dioxide (CO_2), up to 6% oxygen (O_2), hydrogen sulphide (H_2S) and nitrogen, all of which need to be removed to meet pipeline quality specifications. Many of these gas streams also come into the plants at a relatively low pressure, requiring inlet compression.

Existing gas sources that had been shut in or reduced in production because of poor quality include vacuum gathering systems and gas wells with high contaminant level. Despite the improving economics, the producer still need to treat their gas stream in the most efficient and cost-effective manner possible.

1.2   Problem Statement

1.2.1. Problem identification

The separation of CO_2 from mixtures with other gases is a process of substantial industrial importance. Large volumes of natural gas are treated for CO_2 removal. The main reason for removing CO_2 from natural gas is to improve the fuel gas heating value for further usage.

The composition of CO_2 in natural gas may vary from 2 to 80% depending on the geographical location of the well. The removal of CO_2 is very important and the concentration of CO_2 must be below 2% before the gas can be sold. Gas Malaysia specifies an even more stringent level where a maximum 1.83% is to be achieved in the treated stream.

However, the existing methodology for carbon dioxide removal is not sufficient to remove high concentration of CO_2 in our natural gas supply. Therefore, due to the compactness and economic attractiveness of polymeric membrane, membrane gas permeation emerges as an effective alternative to the conventional absorption units.

Mathematical models are very helpful in understanding the mechanism of permeation and separation behaviour for high content CO_2 removal as a function of various process influences such as pressure, concentration, etc. Furthermore, the similar empirical study carried out on a pilot plant scale is both time consuming and expensive. Thus, mathematical models by using Matrix Laboratory (MATLAB) software can generate sets of data concerning the behaviour of the system quickly without involving much cost, as compared to experimental study.

Therefore, by predicting the membrane performance using MATLAB, and by collaborating dual mode model with bulk flux contribution, we might be able to remove higher CO_2 content in natural gas supply.

2

1.2.2. Significance of the Project

A solution to solve the previously stated problem would be useful as to treat the high content of CO_2 which came together with the natural gas supply. This is important to ensure that natural gas can achieve the pipeline quality for further usage. In addition, by using membrane gas separation units, they are smaller than other types of plants as compared to amine stripping plants. Therefore, have relatively small footprints as it is important in environments such as offshore gas-processing platforms.

1.3 Objective(s)

The objectives of the author's research include:

- To develop membrane modelling on separation process based on the intrinsic properties of membrane.
- To predict the membrane separation performance in terms of its selectivity and permeability for the separation of methane and CO_2 with the operating condition of pressure and composition.

1.4 Scope of Study

This project will be utilizing the fundamental knowledge in Fluid Mechanics and Transport Phenomena. The scope is divided into 5 phases:

- Literature review on membranes to select on the type of membrane applied in this study.
- Literature review on the permeability model (dual mode model with bulk flux contribution) that could predict the mechanism of gas permeation in dense polymeric membrane as a function operating pressure and composition.
- From the information obtained, the parameters such as pressure and feed composition to be tested will be determined.
- MATLAB programming will be used for modeling of the membrane.
- Finally, detailed analysis of the findings will be discussed.

3

1.5 Feasibility of Project within Scope and Time frame

This project is feasible in UTP because the main tool required to complete this project, which is MATLAB program is available in the computer laboratory. This research project is carried out for two semesters and the scope are described as below:

The first phase (FYP-1) of the project involves the literature review on current utilization and properties of membrane (6FDA-TADPO polypyrrolone) for natural gas-CO_2 separation as well as the permeability model (dual mode model with bulk flux contribution) that are used to predict the mechanism of gas permeation in the membrane.

The second phase (FYP-II) of project involves MATLAB programming and analysis for the mathematical model that could predict the separation performance of the membrane. Results obtained will be discussed and to be compared with the experimental results obtained in the first part of studies to conclude the project.

With the initiative and enthusiasm in completing this research project, the author believed that two semesters are enough to carry out this project.

CHAPTER 2

LITERATURE REVIEW & THEORY

2.1   Theory

2.1.1   Classification of Membrane Process

There are many types of membrane processes namely:

   a) Gas separation in porous solid

   b) Liquid permeation or dialysis

   c) Gas permeation in a membrane

   d) Reverse osmosis

   e) Ultra filtration and microfiltration membrane process

   f) Gel permeation chromatography

For this project, we are applying the process of gas permeation in a membrane. The membrane which the author is using is dense polymeric organic membrane, specifically 6FDA-TADPO polypyrrolone membrane. The solute gas first dissolves in the membrane and then diffuses in the solid to the other gas phase. Separation of a gas mixture occurs mainly because each type of molecule diffuses at a different rate through the membrane.

2.1.2   Types of Membrane

6FDA-TADPO polypyrrolone membrane is asymmetric polymeric membranes. This type of membrane includes a very thin but dense skin on one side of the membrane supported by a porous substructure. The flux increase of these membranes is thousand times higher than the original membranes.

Polypyrrolone have been identified as materials with high selectivity and permeabilities for CO_2/CH_4 separation (Matsumoto and Xu, 1993; Kim et al., 1988; Kim et al., 1989; Tanaka et al., 1989; Stern et al., 1989; Coleman and Koros, 1990). In addition to high selectivities, polypyrrolone possess high glass transition temperatures (Tg > 2000C). Its

permeation properties, combined with its processability (i.e., solubility in common solvents) make it an attractive candidate for gas separation applications. Furthermore, its mechanical strength and high glass transition temperature, better suit it for more rigorous working environments than other noncelluslosics such as polysulfone.

There are 3 types of equipments for gas permeation, namely flat sheet, spiral wound and hollow fiber membranes. However, in this case, hollow fiber membranes are used to characterize the permeability of the membrane. The modules are easy to fabricate and use and the areas of the membranes are well defined.

2.1.3 Types of Flow in Gas Permeation

2.1.3.1 Types of flow and diffusion gradients

In a membrane process, high pressure feed gas is supplied to one side of the membrane and permeates normal to the membrane. The permeate leaves in a direction normal to the membrane, accumulating on the low-pressure side. Because of the very high diffusion coefficient in gases, concentration gradients in the gas phase in the direction normal to the surface of the membrane are quite small (Geankoplis, 1993). Hence, gas film resistance compared to the membrane resistance can be neglected. This means that the concentration in the gas phase in a direction perpendicular to the membrane is essentially uniform, whether the gas stream is flowing parallel to the surface or is not flowing.

If the gas stream is flowing parallel to the membrane in essentially plug flow, a concentration gradient occurs in this direction. Hence, several cases can occur in the operation of a membrane module. The permeate side of the membrane can be operated so that the phase is completely mixed (uniform) or so that the phase is in plug flow. The high pressure feed side can also be completely mixed or in plug flow. Countercurrent or co-current flow can be used when both sides are in plug flow. Hence, separate theoretical models must be derived for these different types of operation.

2.1.3.2 *Assumptions used and ideal flow patterns*

In deriving theoretical models for gas separation by membranes, we will make some assumptions on the:

a) Isothermal conditions

b) Pressure drop in the feed stream and permeate stream which is negligible

c) Effects of total pressure and/or composition of the gas (negligible)

d) Permeability of each component is constant (no interactions between different components)

The important types of idealized flow patterns are summarized as below:
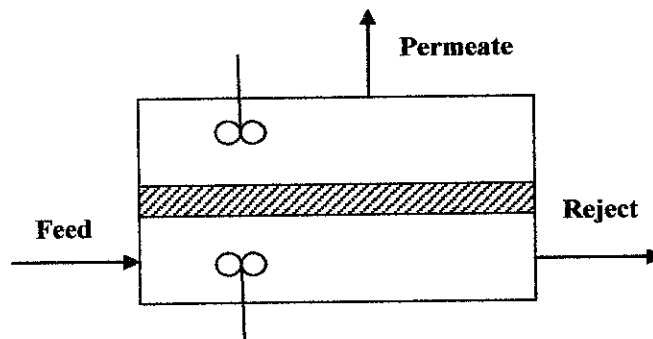
Figure 2.1: Complete mixing model
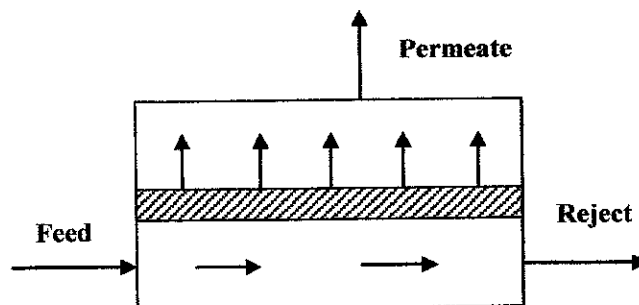
Figure 2.2: Cross-flow model
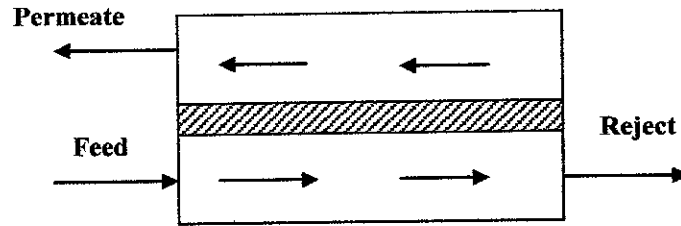
Figure 2.3: Counter-current flow model
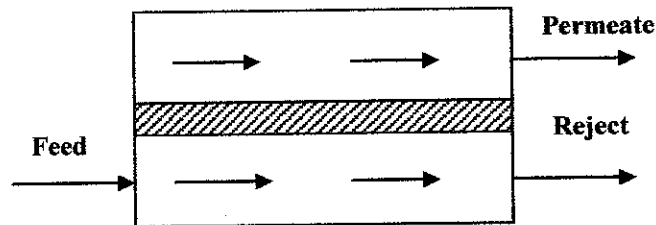
Figure 2.4: Co-current flow model

The complete mixing model assume complete mixing of the binary system either at the feed or permeate side whereas cross flow model assumes no mixing or interaction of the binary system in both feed and permeate sides. In figure (2.2), (2.3) and (2.4), we can see that the feed composition varies along its flow path and the local permeate concentration also varies along the membrane path.

The idealized countercurrent flow model will be the main interest of this research as a starting point for membrane separation modeling.

2.2   Literature review

2.2.1   Model description

In this study, the performance of a membrane is mainly characterized by the selectivity and permeability, or permeance of the components. The preferred productivity measure for asymmetric membranes, which is the permeance (P/l), (the pressure normalized flux) where the actual thickness of the selective skin layer is not clearly measurable. Therefore, by using these parameters, the membrane-based natural gas purification process can be tested.

To determine the base case of the permeances and selectivities of the membrane fibers, the author used binary gas feed. Then, the results obtained from the mathematical model were then compared to understand the separation performance. For the permeation tests, the variables used are feed pressure of 200, 500 and 1000 psi and feed concentration of 20% CO_2/ 80% CH_4, 50% CO_2/ 50% CH_4 and 80% CO_2/ 20% CH_4 feed gas. The optimum operating temperatures used were 308°K as these numbers simulate the concentration at a typical natural gas field.

2.2.2   Modeling of Hollow Fiber Membrane Modules

Undeniably, several mathematical models have been developed for hollow fiber membranes in the literature. Successful membrane modeling and simulation can provide valuable information for the design, optimization and economics of the overall separation process.

Mass, momentum, energy balance equations, appropriate boundary conditions and the relationship governing transport across the membrane are usually included in hollow fiber membrane models. Transport equations describing permeation fluxes across the

9

membrane usually are known to include both molecular diffusion and bulk motion given by equation (2.1) in the case of binary mixtures of A and B.

$$n_A = n_A^{bulk} + n_B^{bulk} \qquad (2.1)$$

Fick's first law of diffusion describes the diffusion transport through a pore-free polymeric medium. Equation (2.1a) and (2.1b) shown below are the diffusion and the bulk transport equations for component A respectively.

$$n_A^{diff} = -\rho D_{Am} \frac{d\omega_A}{dx} \qquad (2.1a)$$

$$n_A^{bulk} = (n_A + n_B + n_P)\omega_A \qquad (2.1b)$$

$$n_A = n_A^{bulk} + n_A^{diff} \qquad (2.1c)$$

$$n_A = (n_A + n_B + n_P)\omega_A - \rho D_{Am} \frac{d\omega_A}{dx} \qquad (2.1d)$$

Where:

D_{Am} (cm2/s) - effective diffusivity of A in the membrane medium

n_i (g/cm2.s) - mass flux of permeant i with respect to a fixed frame of reference

w_i (g/g)   - mass fraction composition of permeant i in the membrane

n_p - mass flux of the polymer (zero at steady state since the membrane is stationary (Kamaruddin and Koros, 1997).

In the simulations of hollow fiber separators the contribution of bulk flow conditions is generally neglected. This assumption is completely reasonable in the cases when the sorption amount of penetrants, w_A and w_B, are negligible such as the sorption of simple gases H_2, He, O_2, and N_2.

10

However, in a recent study, Kamaruddin and Koros (1997) have shown that for CO_2/CH_4 separation using 6FDA-TADPO polypyrrolones and phenol/water separation using polyetherblock-polyamide membranes bulk contributions are significant. Paul and Ebra-Lima (1975 I, II & III) have also shown the importance of the bulk flux term in single component permeation in a highly swollen membrane.

Nevertheless, to the best of our knowledge, studies concerning the frame of reference effects on hollow fiber modules have not been reported in the literature.

Thus, the purpose of this study is to look into the influence of bulk flux contribution on the performance of 6FDA-TADPA polypyrrolone membrane separators and discusses the CO_2/CH_4 separation in membranes.

This model can also be extended to multi-component mixtures, however for the present case, the binary separation of CO_2 and CH_4 illustrates the key points involved and is considered the first step for more realistic models.

The dual mode model has been used to simulate the permeation of multicomponent components in hollow fiber membranes as shown by Thundyil et al. (1999). Chern at al. (1985) presented a bicomponent model on hollow fiber membranes using the dual mode model. Taveria et al. (2001) also presented a multicomponent model on hollow fiber membranes accounting for the permeability pressure and composition dependence according to the dual mode model.

2.3   Model Development

The author proposed a model which considers hollow fiber module for the counter-current configuration. For CO_2/CH_4 separation, the CO_2/CH_4 feed gas enters the module where it is separated into a permeate stream and a retentate stream. The membrane acts as a CO_2 permselective barrier, therefore CO_2 is concentrated in the permeate stream and CH_4 is concentrated in the retentate stream.

11

A one-dimensional mathematical model is solved for the case of dual mode sorption with bulk flux contribution and transport description of permeation in glassy polymers, thus, allowing concentration dependence of the effective diffusion and sorption coefficients. The following are the assumptions made for the model:

- Negligible plasticization as 6FDA-TADPO polypyrrolone is known to be good in resisting CO_2 plasticization.
- It is operated in a steady state condition.
- Isothermal operation (at T=308 K).
- Pressure change in the shell side is negligible.
- Resistance of the porous support is negligible.
- Resistance of the shell and the tube side boundary layers is negligible.
- Uniform flow distribution within the module.
- No defects in the separating layer.
- Constant membrane density.

According to these assumptions, the steady-state mass balance equations for species i, on both the retentate and the permeate sides, are given by;

$$\frac{dR_{Ri}}{dz} = -N_i \qquad (2.2)$$

$$\frac{dR_{Pi}}{dz} = -N_i \qquad (2.3)$$

Where:

Ri - axial molar flow rates of species i on the retentate side

Pi - axial molar flow rates of species i on the permeate side

Z - axial direction.

The pressure on the shell side Rp is assumed constant and equal to the feed pressure.

The membrane is divided up into a predetermined number of stages, M small enough that the pressure and composition gradients are almost constant in each element. The first stage is at the feed end and the Mth stage is at the residue end. The driving force is assumed constant over each of the stages considered. At each stage, the radial permeation fluxes of species i, Ni, must be determined by solving the multicomponent mixture permeation relations. Curvature effects can be neglected and the problem can be solved in cartesian coordinates since the membrane thickness is very small with respect to the radius of the fiber. The multicomponent mixture permeation system comprises 'NC' components and the polymer as shown below;

$$N_1 = -\rho D_1 \frac{d\omega_1}{dx} + \omega_1 \left(\sum_{j=1}^{nc} n_j + n_P \right)$$

$$\ldots$$

$$\ldots$$

$$N_{nc} = -\rho D_{nc} \frac{d\omega_{nc}}{dx} + \omega_{nc} \left(\sum_{j=1}^{nc} n_j + n_P \right) \qquad (2.4)$$

$$N_P = -\rho D_P \frac{d\omega_P}{dx} + \omega_P \left(\sum_{j=1}^{nc} n_j + n_P \right)$$

Paul in the context of diffusion thru elastomeric membranes, noted that the mass flux of the polymer N_p is zero at steady state since the membrane is stationary (Paul and Ebra-Lima, 1975 I, II & III). The mass flux of component j can be obtained by integrating Equation (2.4) with the following boundary conditions;

13

$$x = 0; \quad \omega_1 = \omega_{10} \ \cdots \ \cdots \ \omega_{nc} = \omega_{nc0}$$

$$x = l; \quad \omega_1 = \omega_{1l} \ \cdots \ \cdots \ \omega_{nc} = \omega_{ncl} \qquad (2.5)$$

2.4   Numerical Solution

As mentioned earlier, constant density is assumed within the membrane and average effective diffusion coefficients is evaluated between the upstream and downstream conditions; Kamaruddin and Koros (1997) analyzed the situation for a binary feed. Extending this analysis to multicomponent feeds with 'NC' components results in Eq (2.6);

$$n_j l = \frac{\rho D_{Dj} \ln \left[\dfrac{r_j - \omega_{j2} \sum_{i=1}^{nc} r_i}{r_j - \omega_{j1} \sum_{i=1}^{nc} r_i} \right]}{\sum_{i=1}^{nc} \dfrac{r_i}{r_j}} \qquad (2.6)$$

where r_j and r_i are given by;

$$r_j = \frac{n_j}{n_{ref}}$$

$$r_i = \frac{n_i}{n_{ref}} \qquad (2.7)$$

where

n_{ref} - reference component (can be taken to be equal to the mass flux of the slowest component in the mixture)

The fraction of the bulk flux contribution of component j, *bulk j*, is the ratio of the mass flux of component j due to bulk flow relative to the total mass flux as shown in Equation (2.8). Since the mass fraction of component j, w_j is decreasing in the direction of the mass flux, an average mass composition, $w_{j\,avg}$, should be used in Equation (2.8) when estimating the fraction of the bulk flux contribution.

$$\prod_j^{bulk} = \frac{\omega_j^{avg}\sum_{i=1}^{nc} n_i}{n_j} = \omega_j^{avg}\sum_{i=1}^{nc}\frac{r_i}{r_j} \quad (2.8)$$

Where:

$w_{j\,avg}$ - average mass composition

bulk j - the ratio of the mass flux of component j due to bulk flow relative to the total

   mass flux

Average mass composition in the membrane of component j can be calculated as follows;

$$\omega_j^{avg} = \frac{\int_0^1 \omega_j(x)dx}{\int_0^1 dx} \quad (2.9)$$

where $w_j(x)$ is mass fraction profile of component j in the membrane and is a function of position and can be calculated with the following boundary conditions;

$$x = 0; \quad \omega_1 = \omega_{10} \ldots \ldots \omega_{nc} = \omega_{nc0}$$

$$x = x; \quad \omega_1 = \omega_1(x)\ldots \ldots \omega_{nc} = \omega_{nc}(x) \quad (2.10)$$

15

By integrating we have,

$$\omega_j(x) = \frac{1}{\sum_{i=1}^{nc} \frac{r_i}{r_j}} \left[1 - \left[1 - \omega_{j1} \sum_{i=1}^{nc} \frac{r_i}{r_j} \right] exp \left[\frac{n_j \sum_{i=1}^{nc} \frac{r_i}{r_j} x}{\rho D_{Dj}} \right] \right] \qquad (2.11)$$

However, when the local mass composition, $w_j(x)$ is averaged over the membrane thickness we acquire;

$$\omega_j^{avg} = \frac{1}{\sum_{i=1}^{nc} \frac{r_i}{r_j}} \left[1 - \left[1 - \omega_{j1} \sum_{i=1}^{nc} \frac{r_i}{r_j} \right] \frac{\rho D_{Dj}}{n_j l \sum_{i=1}^{nc} \frac{r_i}{r_j}} \left[exp \left[\frac{n_j l \sum_{i=1}^{nc} \frac{r_i}{r_j}}{\rho D_{Dj}} \right] - 1 \right] \right] \qquad (2.12)$$

By substituting Equation (2.12) into Equation (2.8), we can obtain the bulk flux contribution of component j:

$$\prod_j^{bulk} = \left[1 - \left[1 - \omega_{j1} \sum_{i=1}^{nc} \frac{r_i}{r_j} \right] \frac{\rho D_{Dj}}{n_j l \sum_{i=1}^{nc} \frac{r_i}{r_j}} \left[exp \left[\frac{n_j l \sum_{i=1}^{nc} \frac{r_i}{r_j}}{\rho D_{Dj}} \right] - 1 \right] \right] \qquad (2.13)$$

The permeance Q, of component j on stage k is defined as the permeability P, divided by the skin layer thickness. Permeability can be obtained by normalizing the mass flux, diffusional or total (bulk and diffusional) flux, with the thickness and driving force (partial pressure or fugacity difference), and can be written for component j on stage k as follows;

$$Q_{j,k} = \frac{P_{j,k}}{l} = \frac{22400 \, n_{j,k} \, l}{MW_j \left(p_{j,1} - p_{j,2} \right)} \qquad (2.14)$$

16

The molar volume of gaseous penetrants is generally not known. Therefore it is always more convenient to work with the mass flux units. By using Eq. (2.13), the diffusion based permeability, P_j *diff*, can be calculated from the observed permeability, *obs* P_j as follows;

$$P_j^{diff} = (1 - \prod_j^{bulk}) P_j^{obs} \qquad (2.15)$$

From Equation (2.14), the observed permeability can be obtained with the total observed (bulk and diffusion) mass flux. Then, the mass fraction can be calculated using the dual mode model.

The population of the components sorbed in the free volume is referred to as the Langmuir's population while those occupying the dense matrix are referred to as the Henry's population. A companion transport model assigns separate mobilities to the penetrants in the Langmuir and Henry's law populations.

Thus, this model is mathematically equivalent to assuming that only a fraction, F, of the Langmuir's population is able to perform diffusive jumps equivalent to those or the Henry's population for the case of local equilibrium. The 'mobile' concentration of component j is shown in Equation (2.16) using the dual mode transport model.

The mobile mass fraction wj *mobile* is used when describing the permeant transport in glassy polymers.

$$\omega_j^{mobile} = \frac{k_{Dj}p_j M_j}{22400\rho}\left(1 + \frac{F_j K_j}{1 + \sum_{i=1}^{nc} b_j f_j}\right) \qquad (2.16)$$

17

Where:

k_{Dj} - Henry's law constant of component j which characterizes the sorption in the dense region of the polymer matrix

b_j - constant that is a measure of the affinity of the penetrant to the Langmuir sites

F_j - ratio of the diffusion coefficients of Langmuir's population to Henry's populations of component j

f_j - fugacity of component j

The gas phase fugacity of pure and mixed CO2/CH4 can be calculated using the virial equation of state (Prausnitz et al., 1986). The fugacity should be used instead of partial pressure since CO_2/CH_4 is non-ideal mixture. The Kj constant can be calculated by the following equation;

$$K_j = \frac{C'_{Hj} b_j}{k_{Dj}} \qquad (2.17)$$

Where:

C'_{Hj} - Langmuir capacity constant

CHAPTER 3

METHODOLOGY/PROJECT WORK

For the project methodology, it is divided into three important parts, namely:

1) Problem definition

2) Design

3) Evaluation & Verification

Problem definition consists of literature reviews and research regarding current membrane technology, types of membrane, modeling, etc. while design includes the formulation of constraints and objective function. Last but not least, the results obtained from MATLAB simulation is evaluated and verified with experimental data.
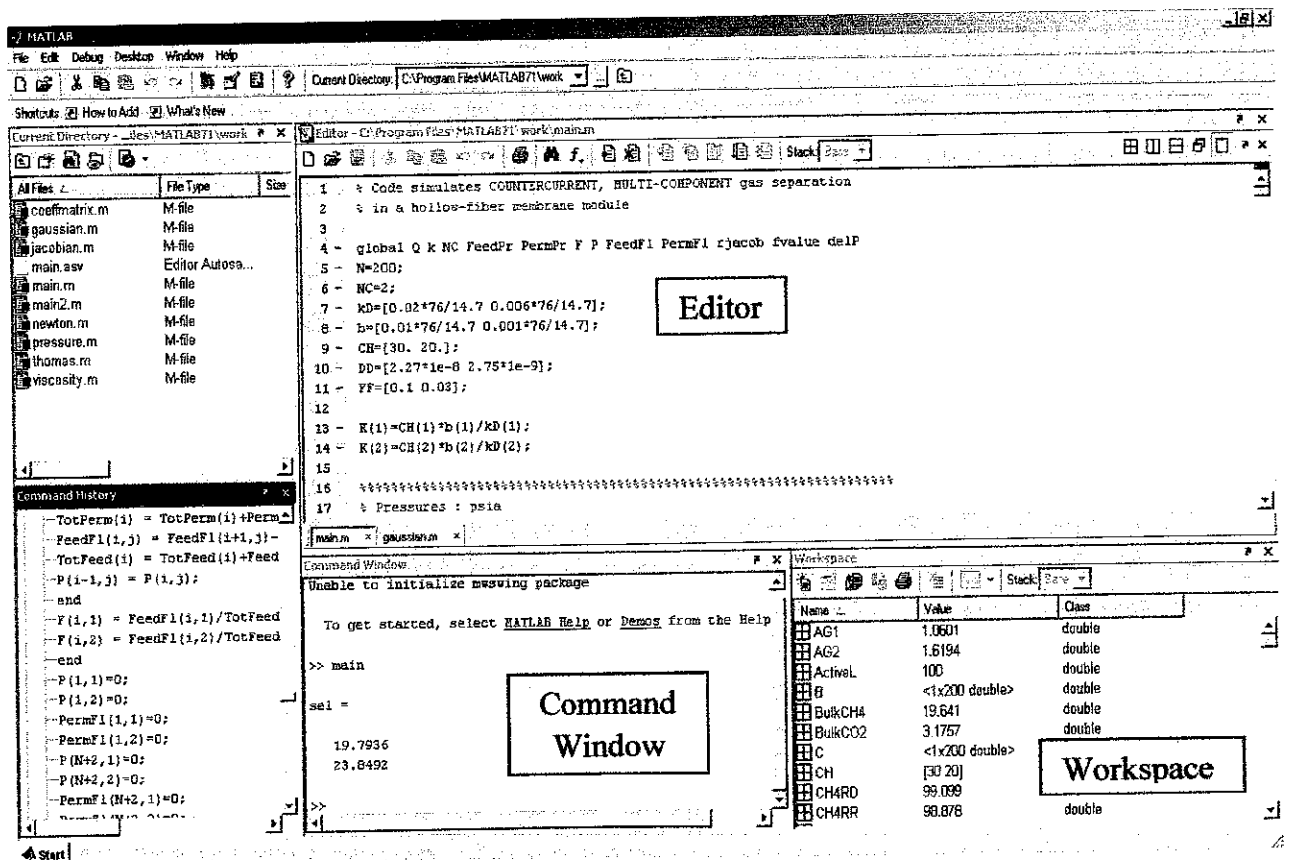
Figure 3.1: MATLAB software used in this project

3.1 Research Methodology

Literature review on the membrane technology of CO_2 removal from natural gas

⬇

Literature review on the type of membrane used in the simulation

⬇

Literature review on type of modeling used in simulation

⬇

Learning on the simulation of MATLAB

⬇

Simulation of the membrane separation for high CO_2 content

⬇

Data collection and verification with experimental result

⬇

End

3.2   Mathematical Modeling Methodology


```
                          ┌─────────┐
                          │  Start  │
                          └─────────┘
                               │
                               ▼
   ┌────────────────────────────────────────────────────────────┐
   │ Read F, D_D, k_D, C'_H, b, FeedFl, FeedPr, PermPr, membrane │
   │ thickness, T, Feed mole fraction, Fiber ID and OD, Fiber    │
   │ active length, Number of fibers,tolr=1d-10,error=10000      │
   └────────────────────────────────────────────────────────────┘
                               │
                               ▼
              ┌────────────────────────────────┐
              │ Call Equation 2.17 to compute K │
              └────────────────────────────────┘
                               │
                               ▼
              ┌────────────────────────────────┐
              │        Call Equation 2.14       │
              │    To compute Q (permeance)     │
              └────────────────────────────────┘
                               │
                               ▼
```

Read F, D_D, k_D, C'_H, b, FeedFl, FeedPr, PermPr, membrane thickness, T, Feed mole fraction, Fiber ID and OD, Fiber active length, Number of fibers,tolr=1d-10,error=10000

Call Equation 2.17 to compute K

Call Equation 2.14
To compute Q (permeance)

Call Equation 2.16 to compute ω_j^{mobile}

Call Equation 2.12 to compute ω_j^{avg}

Call equation 2.13 to compute bulk j

If Error > tolr
(tolerance)

YES

NO

Error
(manipulate
value)

No error

Plot graph

End

3.3   Gantt Chart

Table 3.1: Gantt Chart for FYP 2

No.	Activities	Duration (Weeks)	MAY 1	JUNE 2	JUNE 3	JUNE 4	JUNE 5	JUNE 6	JULY 7	JULY 8	JULY 9	JULY 10	AUGUST 11	AUGUST 12	AUGUST 13	AUGUST 14	SEPTEMBER
1	FYP II Briefing 1	1	■														
2	MATLAB modeling	6	■	■	■	■	■	■									
3	Verification of data collected with experimental data obtained	1							■								
4	FYP II Briefing 2	1							■								
5	Submission of FYP Progress Report	1								■							
7	Detailed results and analysis	4							■	■	■	■					
8	Pre-EDX	1											■				
9	Submission of Draft Report	1												■			
10	Submission of Dissertation (Soft Bound)	1													■		
11	Submission of Technical Paper	1														■	
12	Oral Presentation	1															■
13	Submission of Dissertation (Hard Bound)	1															■

■ Fixed Dates
■ Planned Dates

Legends

B = Mid Sem Break

E= Final Examination

H=Semester Break

22

3.4 Research and Analysis Technique

Research technique in Final Year Project I will be mainly based on literature review of journals, conference, reports and internet sources to get a main idea of this project as well as start-up of MATLAB one dimensional modeling to study the permeability of natural gas. As for Final Year Project II, the author will go into more detail in dual-mode sorption model with bulk flux contribution by using MATLAB program to identify the hollow fiber membrane separation performance.

3.5 Tools Required

Hardware

As this is a modeling type of project, the author would need a good computer for the modeling work.

Software

Table 3.2: Software used in this study

No.	Software	Part	Details
1	MATLAB	Modeling	• For plotting of functions and data, numerical computing, graphical multi-domain simulation and model-based design for dynamic and embedded systems.
2	Microsoft Office	Documentation/ Presentations	• For calculations, tables, chart, etc.

CHAPTER 4

RESULTS AND DISCUSSION

4.1 Simulation parameters

MATLAB modelling has been done to predict the performance of 6FDA-TADPO polypyrrolone membrane. It is a rigid polymer where its open structure and chain rigidity give it desirable membrane properties which are high permeability and selectivity. These unique properties of the membrane enable it to resist carbon dioxide plasticization better than most other polymers. Therefore it is an ideal example to illustrate the bulk flux effects at high CO_2 pressure without such plasticization complication.

Table 4.1 below shows the dual mode parameters of the 6FDA-TADPO polypyrrolone membrane at 35°C (308°K) while the default parameters for simulation are given in Table 4.2. Although only counter-current flow configuration is considered, similar conclusions can be obtained for co-current configuration.

Table 4.1: Fugacity based dual-mode of CO_2 and CH_4 and partial immobilization parameters of 6FDA-TADPO polypyrrolone for CO_2 and CH_4 at 35°C

	CO_2	CH_4
$F (D_H/D_D)$	0.084	0.026
D_D (cm^{2}s^{-1})	1.196e-7	1.12e-8
k_D (cm^3 (STP) cm^{-3} atm^{-1})	1.526	0.327
C'_H (cm^3 (STP) cm^{-3})	34.084	22.838
b (atm^{-1})	1.023	0.160

(Reference: Adapted from Kamaruddin and Koros (1997))

24

Table 4.2: Default parameters for simulations

Parameter	Default value
Thickness of membrane	0.1 micron
Feed flow rate	50 000 SCFH
Feed pressure	200 psia
Permeate pressure (at exit)	20 psia
Temperature	308 K
Feed mole fraction	50/50 CO_2/CH_4
Fiber OD	250 microns
Fiber ID	125 microns
Fiber active length	100 cm
Number of fibers	300 000

Through Matlab, the author inserted the coding for the equations mentioned earlier and the graphs plotted are observed and analyzed. Here, the effect of CO_2 feed mole fraction towards CO_2/CH_4 selectivity, CO_2 average concentration inside the membrane, CO_2 bulk flux contribution and the simulation of CO_2 permeance for 50/50 CO_2/CH_4 feed will be analyzed.

4.2   Effect of CO₂ mole fraction
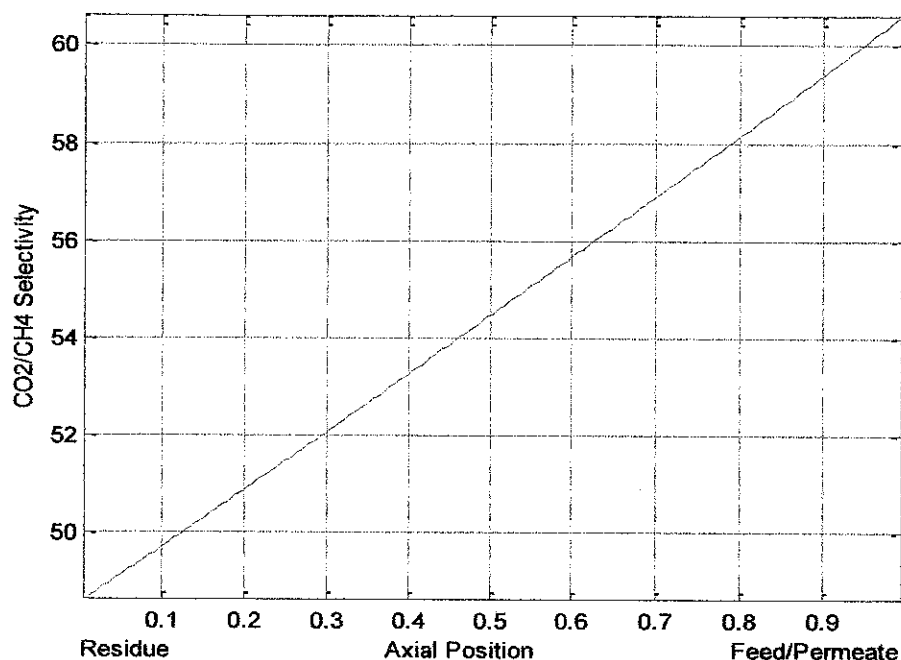
Figure 4.1: Effect of CO₂ feed mole fraction on 50/50 CO₂/CH₄ selectivity
(from MATLAB)
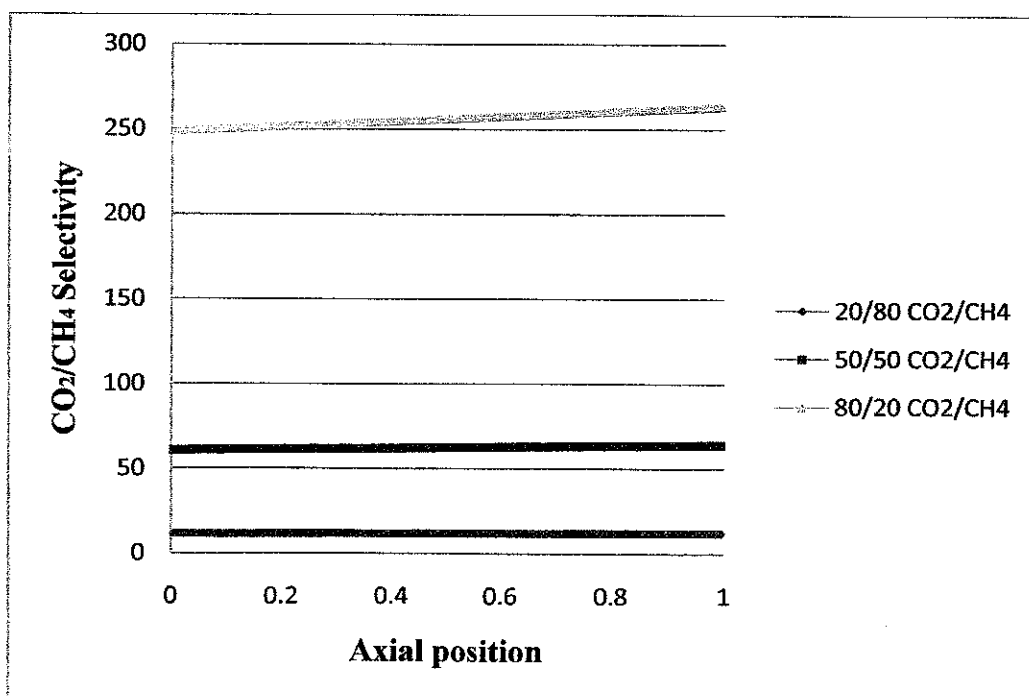
Figure 4.2: Effect of CO₂ / CH₄ selectivity towards different feed composition

26

As shown in Figure 4.1 and Figure 4.2, the CO_2 feed mole fraction has a significant impact on the bulk flux contribution of CO_2 and CH_4. When the feed composition is increasing from 20/80 CO_2/CH_4 to 80/20 $CO_2/CH4$, the selectivity increases. Therefore, increasing the faster component, which is the CO_2 feed-side mole fraction, increases the CO_2/CH_4 selectivity.
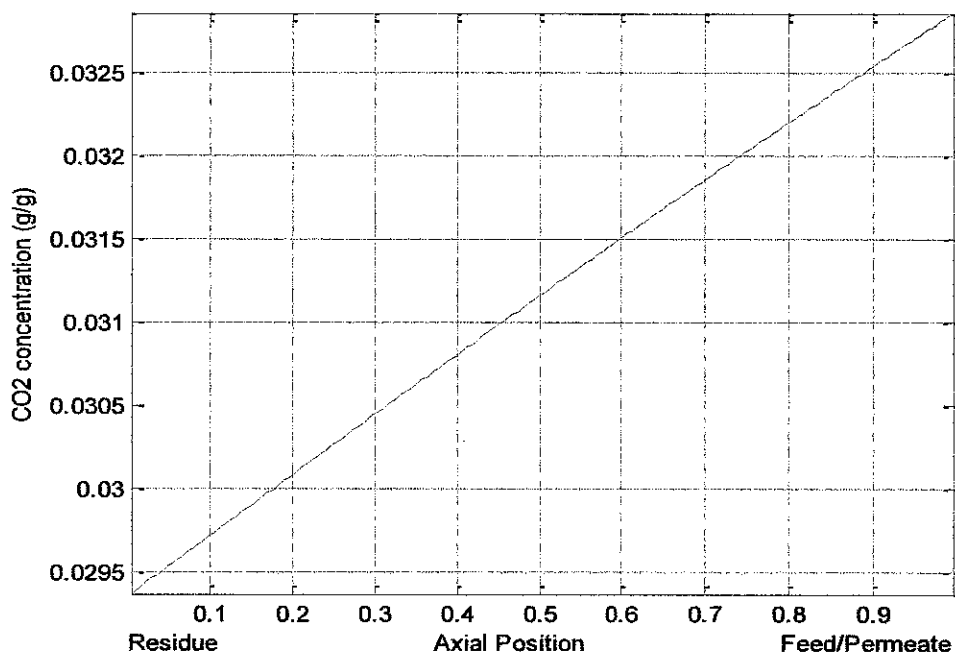
Figure 4.3: Effect of CO_2 feed mole fraction on CO_2 average concentration inside the membrane (from MATLAB)
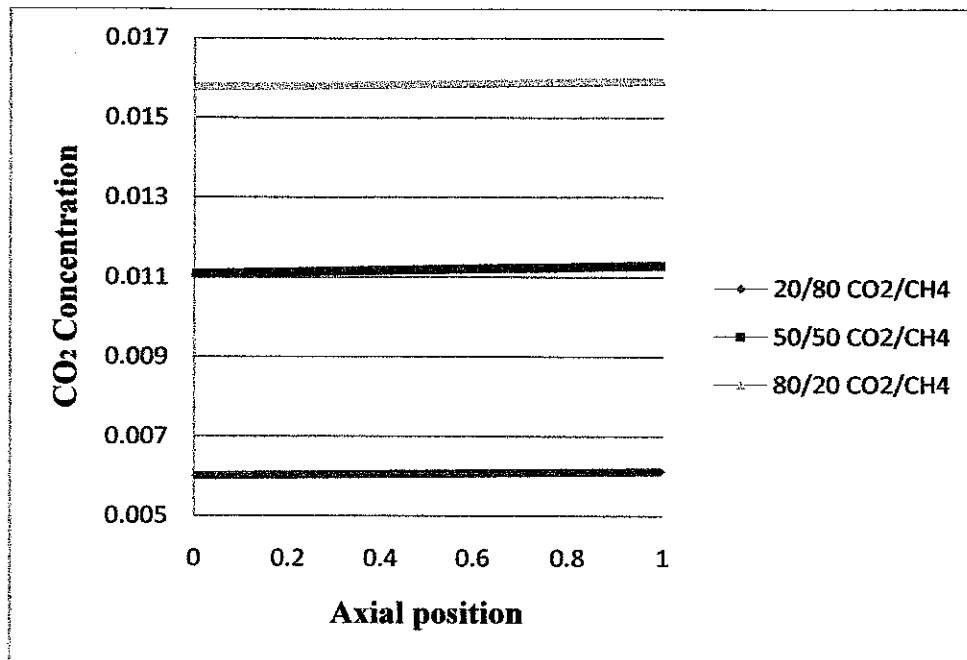
Figure 4.4: Effect of CO2 concentration towards different feed composition

By increasing the CO_2 mole fraction increases also the CO_2 sorption levels in the membrane but at the same time, decreases the CH_4 sorption levels in the membrane from the dual mode and competitive sorption standpoint. Figure 4.3 shows the CO_2 concentration profile along the membrane for the 50/50 CO_2/CH_4 mixtures.

As can be seen, the CO_2 concentration decreases from the feed/permeate side to the residue side because the CO_2 is selectively permeating to the low-pressure side of the membrane.
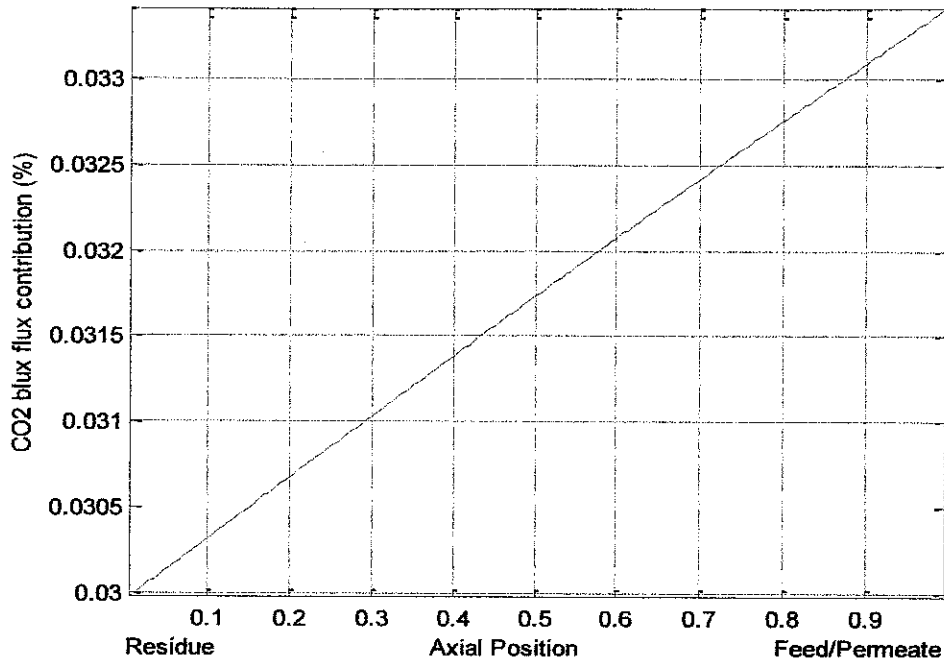
Figure 4.5: Effect of CO_2 feed mole fraction on CO_2 bulk flux contribution (from MATLAB)
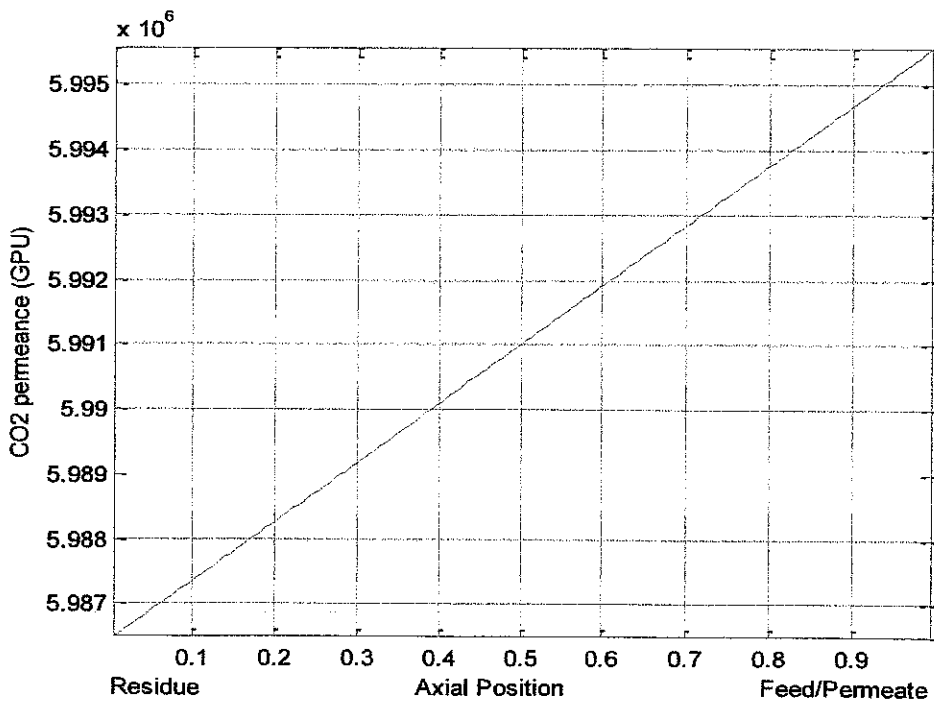

Figure 4.6: Simulation of CO_2 permeance for 50/50 CO_2/CH_4 feed (from MATLAB)

As the CO_2 concentration in the feed side decrease, it will cause the CH_4 concentration to increase. Same goes to the average concentration of CO_2 and CH_4. Although selectivity and average concentration of CH_4 will have opposite effects, the bulk flux contribution of CH_4 is still significant relative to the diffusional flux of CH_4.

The bulk flux contribution of CH_4 is more sensitive to the CO_2/CH_4 selectivity than the bulk flux contribution of CO_2 because bulk flux contribution of CO_2 is proportional to 1/r (r represents selectivity) while the bulk flux contribution of CH_4 is proportional to r. Therefore, when one component is much faster than the other component, the slower component is "swept" along by the faster component. Therefore, the bulk flux of CH_4 cannot be neglected.

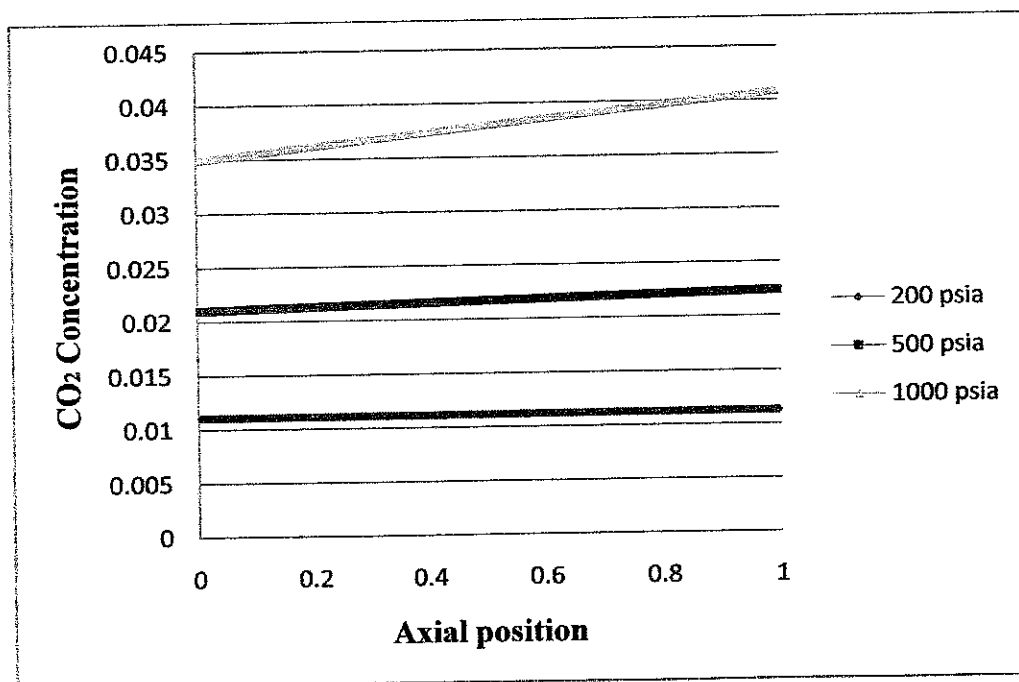## 4.3 Effect of feed pressure

Figure 4.7: Effect of CO_2 concentration towards different feed pressures

30

Figure 4.7 shows the effect of increasing the total feed pressure for the 50/50 gas mixture on the total CO_2 and CH_4 concentration in the membrane. As we can see, the average CO_2 concentration decreases along the membrane length from the feed side to the retentate side. However, there was little dependence on pressure because of the competitive nature of sorption shown in the case of 200 and 500 psi feed pressures. This can be explained in terms of the dual mode model. At low feed pressures, the average concentration of CH_4 comprised of both the Henry's and Langmuir modes, which both have opposite effects on CH_4 sorption. At high feed pressures, the average concentration of CH_4 is dominated by the Henry's mode only.
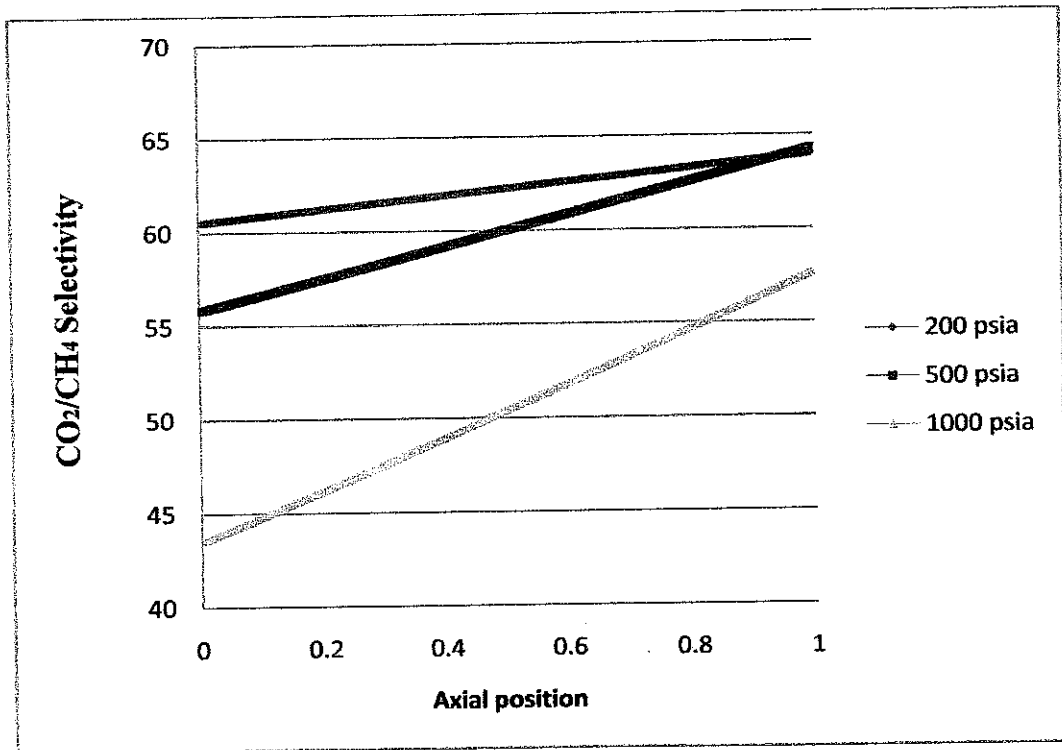

Figure 4.8: Effect of CO_2 / CH_4 selectivity towards different feed pressure

4.4   Validation of simulation results

Validation of results is essential to ensure the accuracy of this mathematical model. The data extracted from the MATLAB modeling is as follows:

Table 4.3: Values from MATLAB model

CH_4 feed fugacity (psi)	CO_2/CH_4 Selectivity
70	57.68
220	53.87
290	50.82
380	47.64
440	45.30

The data above will then be compared with the experimental data which has already been done extracted from literature review [4].

Table 4.4: Experimental data

CH_4 feed fugacity (psi)	CO_2/CH_4 Selectivity
70	54
220	49
290	47
380	45
440	43

(Reference: Adapted from Kamaruddin and Koros (1997))

Figure 4.10 below plots the experimental and MATLAB model data for comparison to validate and for further error calculations.
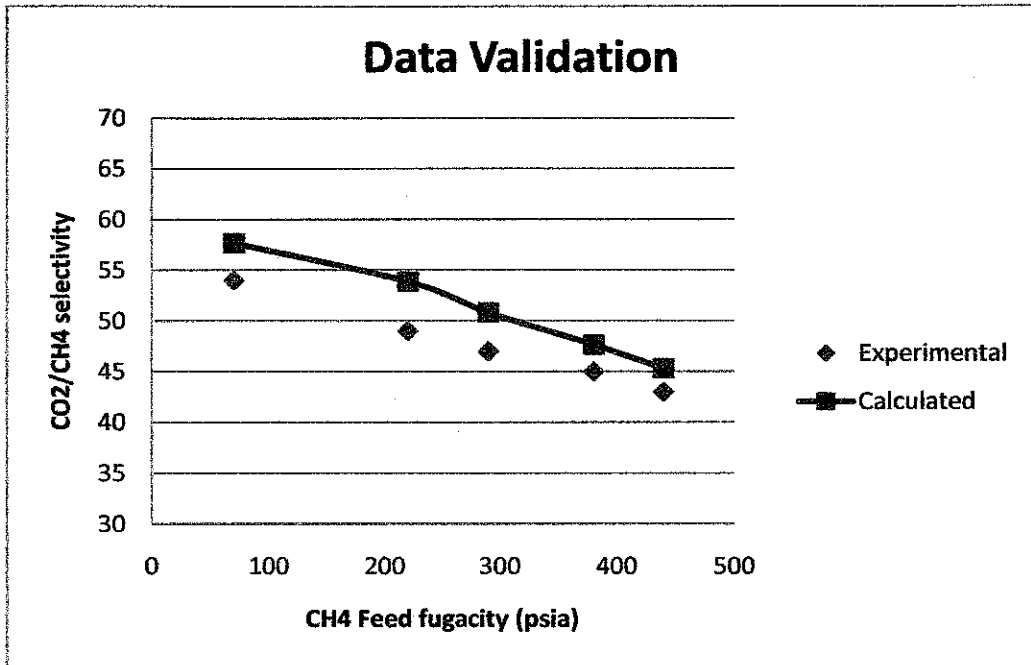
Data Validation

Figure 4.10: Plot of experimental and modeling data

The errors calculated are shown below:

Table 4.5: Error calculation

CH4 feed fugacity (psi)	% Error
70	6.8148148
220	9.9387755
290	8.1276596
380	5.8666667
440	5.3488372

Thus, the average % error is:

$$Average \% \ Error = \frac{6.81 + 9.94 + 8.13 + 5.87 + 5.35}{5}$$

$$= 7.22 \%$$

Therefore, the results from Matlab are considered accurate with 6 to 12% margin of error.

CHAPTER 5

CONCLUSION & RECOMMENDATION

The separation of CO_2 from mixtures with other gases is a process of substantial industrial importance. Further analysis and research have to be carried out to remove high content of carbon dioxide and to achieve pure, clean natural gas. Literature review on the types of membrane, permeability model that could predict the mechanism of gas permeation in dense membrane as a function of operating pressure and composition is analyzed.

When modelling hollow-fiber membrane modules, it is common to neglect the bulk term in the transport equations. However, Dual-mode sorption model with bulk flux contribution which is used in this project has proven that this simplification may imply incorrect estimation of the membrane modules performance and it is particularly critical for systems with high CO_2 partial pressure in the feed-side.

Better feasibility study such as the effect of membrane thickness and area, permeate pressure, etc is needed to further confirm that this model is the perfect solution for CO_2 removal from natural gas using membrane. In additional, this model can also be extended to multi-component mixtures to predict the separation performance of heavy hydrocarbons, hydrogen sulphide and so on.

REFERENCES

[1]   D. Raucher, M. Sefcik, "Industrial gas separation", ACS Symp. Ser. 111 (1983)
       223.

[2]   Keshavarz, P., S. Ayatollahi, et al. (2008). "Mathematical modeling of gas-liquid
       membrane contactors using random distribution of fibers." Journal of Membrane
       Science 325(1): 98-108.

[3]   Kumar, P. S., J. A. Hogendoorn, et al. (2002). "New absorption liquids for the
       removal of CO_2 from dilute gas streams using membrane contactors." Chemical
       Engineering Science 57(9): 1639-1651.

[4]   H. Denny Kamaruddin, William J. Koros (1997). "Some observations about the
       application of Fick's first law for membrane separation of multicomponent
       mixtures." Journal of Membrane Science 135: 147-159.

[5]   Thundyil, M. J. and W. J. Koros (1997). "Mathematical modeling of gas
       separation permeators -- for radial crossflow, countercurrent, and concurrent
       hollow fiber membrane modules." Journal of Membrane Science 125(2): 275
       -291.

[6]   Safari, M., A. Ghanizadeh, et al. (2009). "Optimization of membrane-based
       CO_2-removal from natural gas using simple models considering both
       pressure and temperature effects." International Journal of Greenhouse
       Gas Control 3(1): 3-10.

[7]   Sohrabi, M. R., A. Marjani, et al. (2011). "Mathematical modeling and numerical simulation of CO2 transport through hollow-fiber membranes." Applied Mathematical Modelling 35(1): 174-188.

[8]   Thundyil, M. J. and W. J. Koros (1997). "Mathematical modeling of gas separation permeators -- for radial crossflow, countercurrent, and cocurrent hollow fiber membrane modules." Journal of Membrane Science 125(2): 275-291.

[9]   W.R. Vieth, J.M. Howell, J.H. Hsieh, Dual sorption theory, J. Membr. Sci. 1 (1976) 177.

[10]   Jin-Sheng Wang, Yoshinori Kamiya, et al. (1998). "A method of validation and parameter evaluation for dual-mode sorption model." Journal of Membrane Science 154(1999): 25-32.

[11]   Rajiv Mahajan, Catherine M, William J., et al. (1999). "Polymer Membranes for gas and vapor separation." ACS Symposium Series Vol. 733.

[12]   A.F. Ismail, W. Lorna et al. (2002). "Penetrant-induced plasticization phenomenon in glassy polymers for gas separation membrane." Journal of Membrane Science 27(2002): 173-194.

[13]   Wind, J. D., D. R. Paul, et al. (2004). "Natural gas permeation in polyimide membranes." Journal of Membrane Science 228(2): 227-236.

[14]   Yegani, R., H. Hirozawa, et al. (2007). "Selective separation of CO2 by using novel facilitated transport membrane at elevated temperatures and pressures." Journal of Membrane Science 291(1-2): 157-164.

[15] G.R. Mauze, S.A. Stern, The dual-mode solution of vinyl chloride monomer in poly(vinyl chloride), J. Membr. Sci. 18 (1984) 99.

[16] S. Zhou, S.A. Stern, The effect of plasticization on the transport of gases in and through glassy polymers, J. Polym. Sci. Part B: Polym. Phys. 27 (1989) 205.

APPENDICES

A.1   MATLAB coding

```
% Code simulates COUNTERCURRENT, MULTI-COMPONENT gas separation
% in a hollow-fiber membrane module

global Q k NC FeedPr PermPr F P FeedFl PermFl rjacob fvalue delP
N=200;
NC=2;
kD=[0.02*76/14.7 0.006*76/14.7];
b=[0.01*76/14.7 0.001*76/14.7];
CH=[30. 20.];
DD=[2.27*1e-8 2.75*1e-9];
FF=[0.1 0.03];


K(1)=CH(1)*b(1)/kD(1);
K(2)=CH(2)*b(2)/kD(2);


%% Pressures : psia
for i=1:N+2,
    FeedPr(i) = 200.;
    PermPr(i) = 20;
end


%% Temperatures : Kelvin
T = 308.0;

% Flow rates : cc-STP/sec (SCFH*7.43)
for i=1:N+2,
    TotFeed(i)=0.0;
    TotPerm(i)=0.0;
end
TotFeed(N+2) = 50000.0*7.43;

% Feed Composition : mole fraction and flow rate
F(N+2,1) = 0.50;
F(N+2,2) = 0.50;
FeedFl(N+2,1) = F(N+2,1)*TotFeed(N+2);
FeedFl(N+2,2) = F(N+2,2)*TotFeed(N+2);

% input shell-side(1) or bore-side feed(2)
nval = 1;

%% FIBER DATA
DENS=1.405;
Nfibers = 300000;
t=0.5*1d-4;

% Fiber dimensions : centimeters (microns*1e-4)
DO = 250.0*1D-4;
DI = 125.0*1D-4;
```

```
%Active fiber length : centimeters
ActiveL = 100.0;
dz = ActiveL/N;


% Mass transfer area per stage
delAk = 2*pi*DO/2*ActiveL*Nfibers/N;


%% COMPONENT DATA
% Molecular weights lb/lbmole
MW =[44.00 16.00];


% Critical Temperatures : Kelvin
Tc =[304.2 190.6];


% Critical Pressures : bar
Pc =[73.8 46.0];


% Critical Volumes : cm3/mol
Vc =[94.0 99.0];


% Permeance : cc-STP/cm^2-sec-psia (GPU*1e-6*5.17)
% (1 GPU = 1e-6 cm3-STP / cm2-sec-cm Hg)
for i=1:N+2,
    Q(i,1) = DD(1)*kD(1)/t;
    Q(i,2) = DD(2)*kD(2)/t;
end
sum1 =0;
for j = 1:NC,
    sum1 = sum1 + Q(N+1,j)*F(N+2,j);
end
sum2 = 0;


for j = 1:NC,
    P(N+1,j) = Q(N+1,j)*F(N+2,j)/sum1;
    parF = F(N+2,j)*FeedPr(N+2);
    parP = P(N+1,j)*PermPr(N+1);
    if parP > parF
        P(N+1,j) = F(N+2,j)*FeedPr(N+2)/PermPr(N+1);
    end
sum2 = sum2 + P(N+1,j);
end
if sum2 > 1
    for j = 1:NC,
        P(N+1,j) = P(N+1,j)/sum2;
    end
end


%%%%%%%%%%%%%%%%%%%%% stage calculations begin %%%%%%%%%%%%%%%%%%%%%%%%%%
for i=N+1:-1:2,
    k = i;
    newton;
    TotFeed(i)=0;
    TotPerm(i)=0;
```

```
for j = 1:NC,
PermFl(i,j) = Q(i,j)*delAk*(FeedPr(i+1)*F(i+1,j) -PermPr(i)*P(i,j));
TotPerm(i) = TotPerm(i)+PermFl(i,j);
FeedFl(i,j) = FeedFl(i+1,j)-PermFl(i,j);
TotFeed(i) = TotFeed(i)+FeedFl(i,j);
P(i-1,j) = P(i,j);
end
F(i,1) = FeedFl(i,1)/TotFeed(i);
F(i,2) = FeedFl(i,2)/TotFeed(i);
end


P(1,1)=0;
P(1,2)=0;
PermFl(1,1)=0;
PermFl(1,2)=0;
P(N+2,1)=0;
P(N+2,2)=0;
PermFl(N+2,1)=0;
PermFl(N+2,2)=0;
for i=2:N+1,
     TotPerm(i) = TotPerm(i) + TotPerm(i-1);
end


for iter=1:1000,

% Calculate new feed flow rates
for i=N+2:-1:2,
     for j=1:NC,
          fF(i,j)= F(i,j)*FeedPr(i);
          fP(i,j)= P(i,j)*PermPr(i);
     end
DENF(i)=1+b(1)*fF(i,1)+b(2)*fF(i,2);
DENP(i)=1+b(1)*fP(i,1)+b(2)*fP(i,2);
end
for i=N+2:-1:2,
     for j=1:NC,
wFeed(i,j)=kD(j)*fF(i,j)*MW(j)/(22400*DENS)*(1+FF(j)*K(j)/DENF(i));
wPerm(i,j)=kD(j)*fP(i,j)*MW(j)/(22400*DENS)*(1+FF(j)*K(j)/DENP(i));
end
end
for i=2:N+1,
     for j=1:NC,
          PermFl(i,j)=FeedFl(i+1,j)-FeedFl(i,j);
          PermFl(i,j)=PermFl(i,j)*MW(j)/22400;
     end
end
tolr=1d-10;
iter1=0;
errr=10000.;
while errr > tolr,
iter1=iter1+1;
errr=0;
for ii=2:N+1,
r1(ii)= PermFl(ii,1)/PermFl(ii,2);
AG1=(1-wPerm(ii,1)*(1+1/r1(ii)))/(1-wFeed(ii,1)*(1+1/r1(ii)));
AG2=(1-wPerm(ii,2)*(1+r1(ii)))/(1-wFeed(ii,2)* (1+r1(ii)));
```

```
PermFl(ii,1)=DENS*DD(1)*log(AG1)/(1+1/r1(ii));
PermFl(ii,2)=DENS*DD(2)*log(AG2)/(1+r1(ii));
rvalue(ii)=PermFl(ii,1)/PermFl(ii,2)-r1(ii);
errr = errr + abs(rvalue(ii));
end
end
for ii=2:N+1,
    ta1=(1+1/r1(ii));
    ta2=(1-wFeed(ii,1)*ta1)*DENS*DD(1);
    ta3=ta2/(PermFl(ii,1)*ta1);
    ta4=exp(PermFl(ii,1)*ta1/DENS/DD(1))-1;
    ta5=1/ta1*(1-ta3*ta4);
    wavg1(ii)=ta5;
    bulk(ii,1)=ta1*ta5;
    tb1=(1+r1(ii));
    tb2=(1-wFeed(ii,2)*tb1)*DENS*DD(2);
    tb3=tb2/(PermFl(ii,2)*tb1);
    tb4=exp(PermFl(ii,2)*tb1/DENS/DD(2))-1;
    tb5=1/tb1*(1-tb3*tb4);
    wavg2(ii)=tb5;
    bulk(ii,2)=tb1*tb5;

end
for i=N+1:-1:2,
    deltPr(i,1)=F(i,1)*FeedPr(i)-P(i,1)*PermPr(i);
    deltPr(i,2)=F(i,2)*FeedPr(i)-P(i,2)*PermPr(i);
    Q(i,1)=22400*PermFl(i,1)/(MW(1)*deltPr(i,1))/t;
    Q(i,2)=22400*PermFl(i,2)/(MW(2)*deltPr(i,2))/t;
end
for j=1:NC,
    [B,C,D] = coeffmatrix(TotPerm,TotFeed,PermPr,FeedPr,Q,delAk,j);
    r(N)=-D(N)*FeedFl(N+2,j);
    D(N) = 0.;
    B(1) = 0.;
    [r] = thomas (B,C,D,r);
    for i=2:N+1,
        FeedFl(i,j)=r(i-1);
    end
clear r
end
for i=2:N+1,
    TotFeednew(i) = 0;
    for j=1:NC,
        TotFeednew(i) = TotFeednew(i) + FeedFl(i,j);
    end
end
TotFeednew(N+2) = TotFeed(N+2);

% Calculate new permeate flow rates
PermFl(1,1)=0;
PermFl(1,2)=0;
for i=2:N+1,
    TotPermnew(i) = 0;
    for j=1:NC,

PermFl(i,j)=PermFl(i-1,j)+FeedFl(i+1,j)- FeedFl(i,j);
```

42

```
        end
TotPermnew(i)= TotPermnew(i-1)+TotFeednew(i+1)- TotFeednew(i);
end
TotPermnew(1) = 0;
for i=2:N+1,
    for j=1:NC,
        F(i,j) = FeedFl(i,j)/TotFeednew(i);
        P(i,j) = PermFl(i,j)/TotPermnew(i);
    end
end
for k=N+1:-1:2,
    nv=-1;
    for j=1:NC,
        X(k,j) = P(k,j);
    end
    XPr(k) = PermPr(k);
    Xtotal(k) = TotPermnew(k);
    [Vmix]=viscosity(k,NC,T,MW,Tc,Pc,X);
    [XPr]=pressure(k,NC,T,DI,dz,Vmix,XPr,Xtotal,Nfibers,nv);
    PermPr(k) = XPr(k);
end


% check post-iteration error
errfeed = abs(TotFeednew(2)-TotFeed(2));
errperm = abs(TotPermnew(N+1)-TotPerm(N+1));
ratiof = errfeed/TotFeednew(2);
ratiop = errperm/TotPermnew(N+1);
if ratiof > 1e-8 | ratiop > 1e-8
    for i=N+1:-1:2,
        TotFeed(i) = TotFeednew(i);
        TotPerm(i) = TotPermnew(i);
    end
else
dsumCO2p=0;
dsumCH4p=0;
rsumCO2p=0;
rsumCH4p=0;
for i=N+1:-1:2,
    PermFl(i,1)=FeedFl(i+1,1)-FeedFl(i,1);
    PermFl(i,2)=FeedFl(i+1,2)-FeedFl(i,2);
    dsumCO2p=dsumCO2p+PermFl(i,1)*MW(1)/22400*(1-bulk(i,1));
    dsumCH4p=dsumCH4p+PermFl(i,2)*MW(2)/22400*(1-bulk(i,2));
    rsumCO2p=rsumCO2p+PermFl(i,1)*MW(1)/22400;
    rsumCH4p=rsumCH4p+PermFl(i,2)*MW(2)/22400;
end
dsump=dsumCO2p*22400/MW(1)+dsumCH4p*22400/MW(2);
rsump=rsumCO2p*22400/MW(1)+rsumCH4p*22400/MW(2);
BulkCO2=(rsumCO2p-dsumCO2p)/rsumCO2p*100;
BulkCH4=(rsumCH4p-dsumCH4p)/rsumCH4p*100;
dyCO2=dsumCO2p*22400/MW(1)/dsump;
dyCH4=dsumCH4p*22400/MW(2)/dsump;
ryCO2=rsumCO2p*22400/MW(1)/rsump;
ryCH4=rsumCH4p*22400/MW(2)/rsump;
dse=(dyCO2/dyCH4)/(F(N+2,1)/F(N+2,2));
rse=(ryCO2/ryCH4)/(F(N+2,1)/F(N+2,2));
sel=[rse;dse]
```

```
SCUTR=(rsump)/TotFeed(N+2)*100;
SCUTD=(dsump)/TotFeed(N+2)*100;


CH4RR=(FeedFl(N+2,2)-rsumCH4p*22400/MW(2))/FeedFl(N+2,2)*100;
CH4RD=(FeedFl(N+2,2)-dsumCH4p*22400/MW(2))/FeedFl(N+2,2)*100;
break
end
end
x1=N+2:-1:2;
x2=2:1:N+1;
for i=2:N+2,
    x1(i-1)=(x1(i-1)-2)/(N+2);
    y1(i-1)=F(i,1);
    y2(i-1)=F(i,2);
end

for i=N+1:-1:2,
    x2(i-1)=(x2(i-1)-1)/(N+1);
    PA2(i-1)=P(i,1)*PermPr(i);
    PB2(i-1)=P(i,2)*PermPr(i);
    y5(i-1)=bulk(i,1);
    y6(i-1)=bulk(i,2);
    y7(i-1)=rl(i);
    PA1(i-1)=F(i,1)*FeedPr(i);
    PB1(i-1)=F(i,2)*FeedPr(i);
    term1a(i-1)=DD(1)/(PA1(i-1)-PA2(i-1));
    term1b(i-1)=DD(2)/(PA1(i-1)-PA2(i-1));
    term2a(i-1)=kD(1)*(PA1(i-1)-PA2(i-1));
    term2b(i-1)=kD(2)*(PA1(i-1)-PA2(i-1));
    term3(i-1)=PA1(i-1)/(1+b(1)*PA1(i-1)+b(2)*PB1(i-1));
    term4(i-1)=PA2(i-1)/(1+b(1)*PA2(i-1)+b(2)*PB2(i-1));
    term5a(i-1)=FF(1)*CH(1)*b(1)*(term3(i-1)-term4(i-1));
    term5b(i-1)=FF(2)*CH(2)*b(2)*(term3(i-1)-term4(i-1));

    Pa(i-1)=term1a(i-1)*(term2a(i-1)+term5a(i-1))*14.7/76*1e6/t;
    Pb(i-1)=term1b(i-1)*(term2b(i-1)+term5b(i-1))*14.7/76*1e6/t;
    Q(i,1)=22400*PermFl(i,1)/(MW(1)*deltPr(i,1))/t;
    P(i-1) = Q(i-1)*F(i-1)/sum1;

end

figure;
% remove first and last element from matrix Q because its all zeros
Q = Q(2:end-1,:);
plot(x2,Q(:,1),'b');
hold on;
xlabel('Residue                          Axial Position
Feed/Permeate')
ylabel('CO2 permeance (GPU)')

grid on;
axis tight
hold off;
```
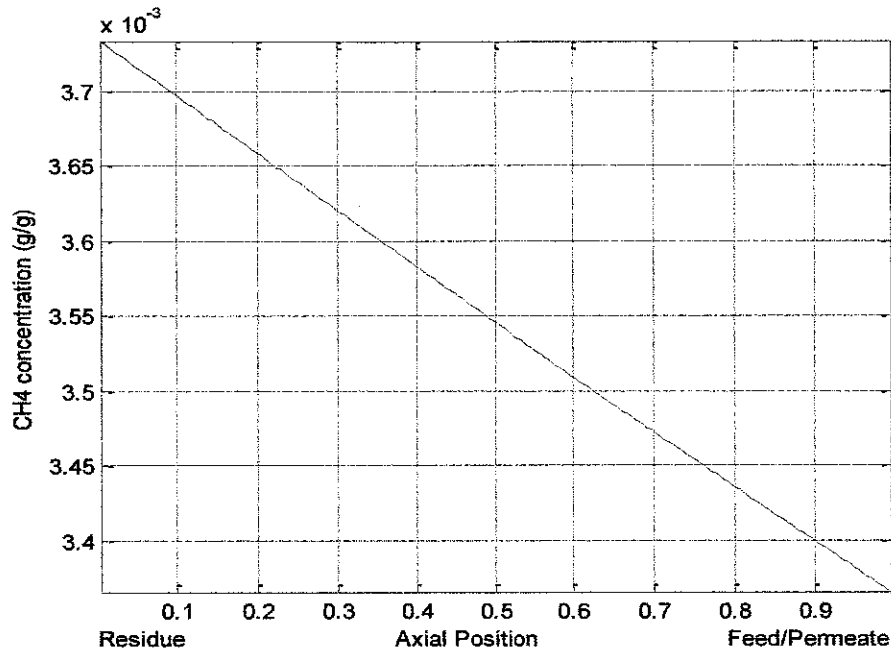
44

A.2   Simulation results

Figure A1: Effect of CO_2 feed mole fraction on CH_4 average concentration inside the membrane
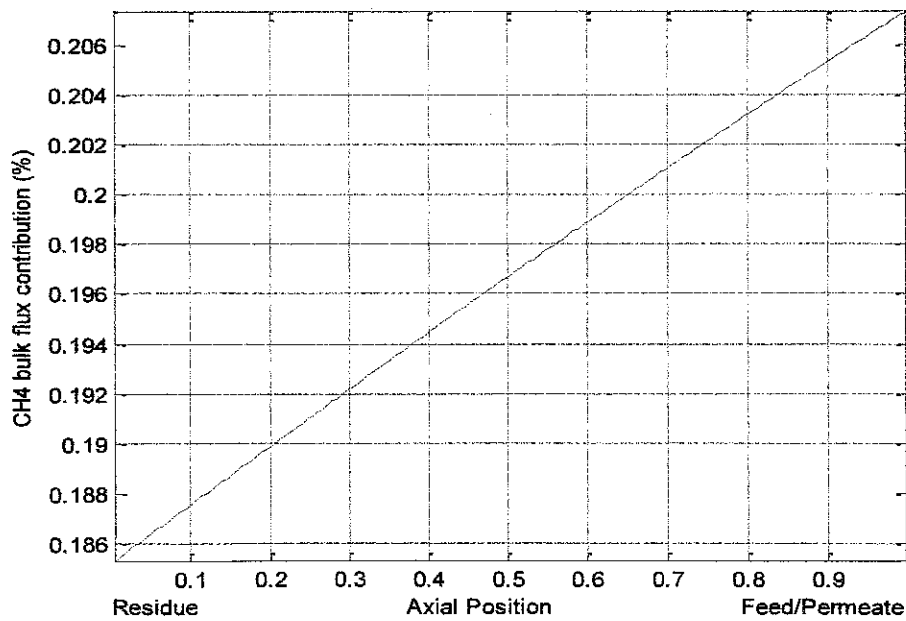

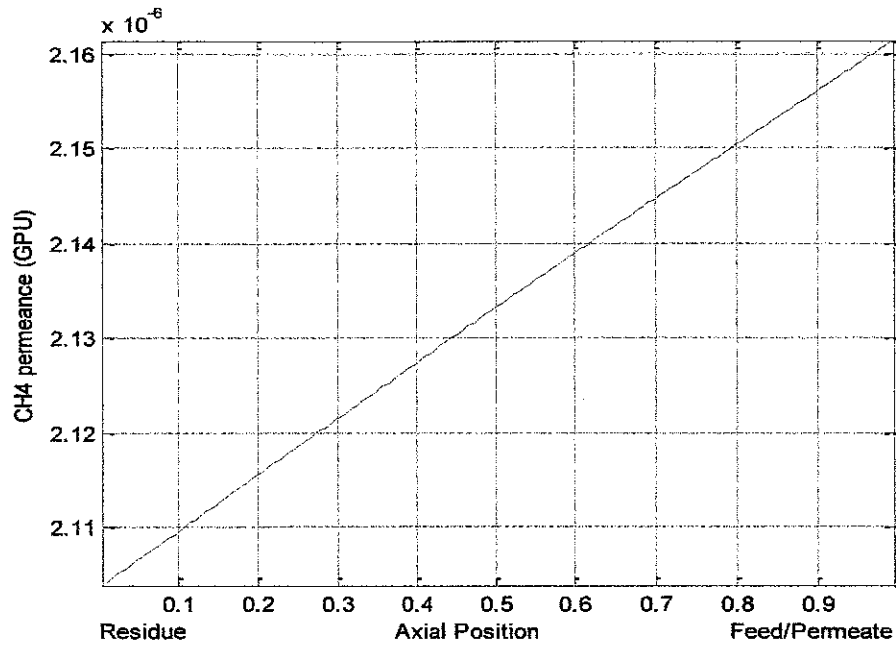Figure A2: Effect of CO_2 feed mole fraction on CH_4 bulk flux contribution

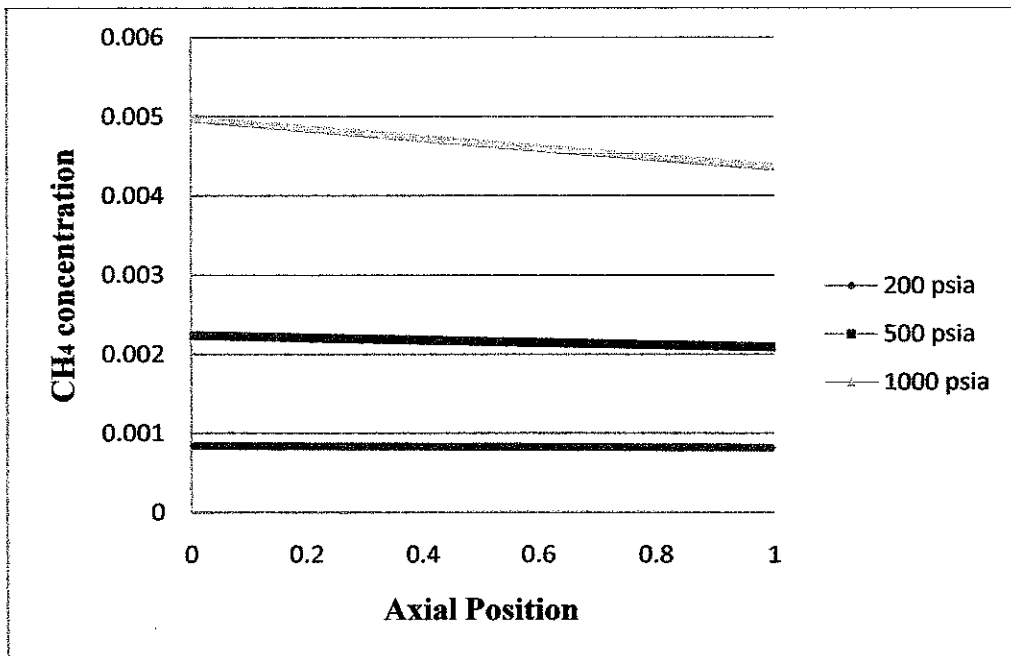Figure A3: Simulation of CH4 permeance for 50/50 CO2/CH4 feed

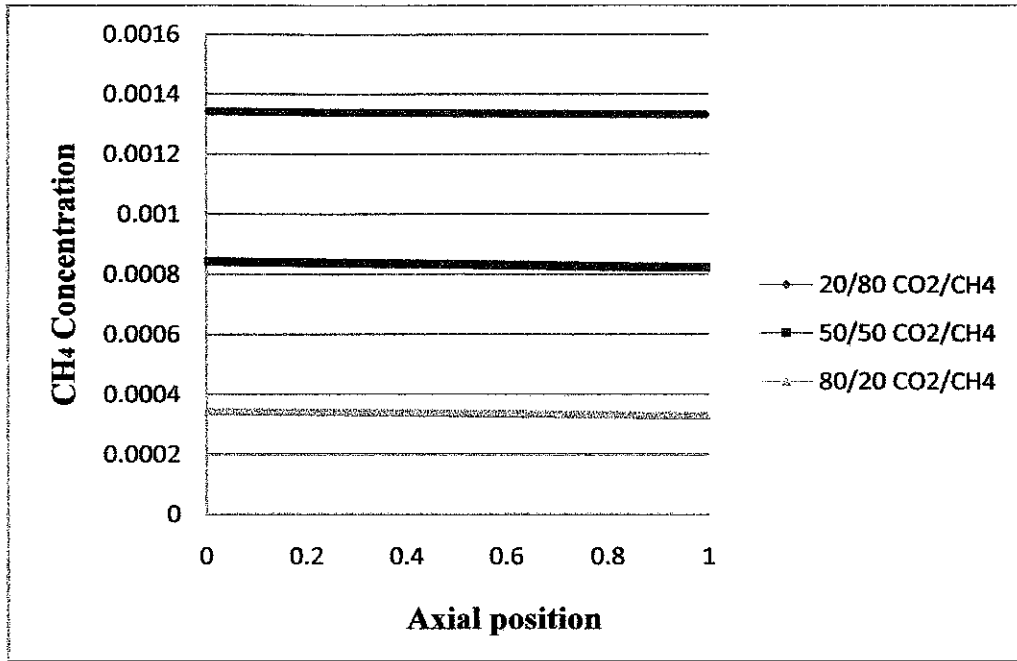Figure A4: Effect of CH4 concentration towards different feed pressure

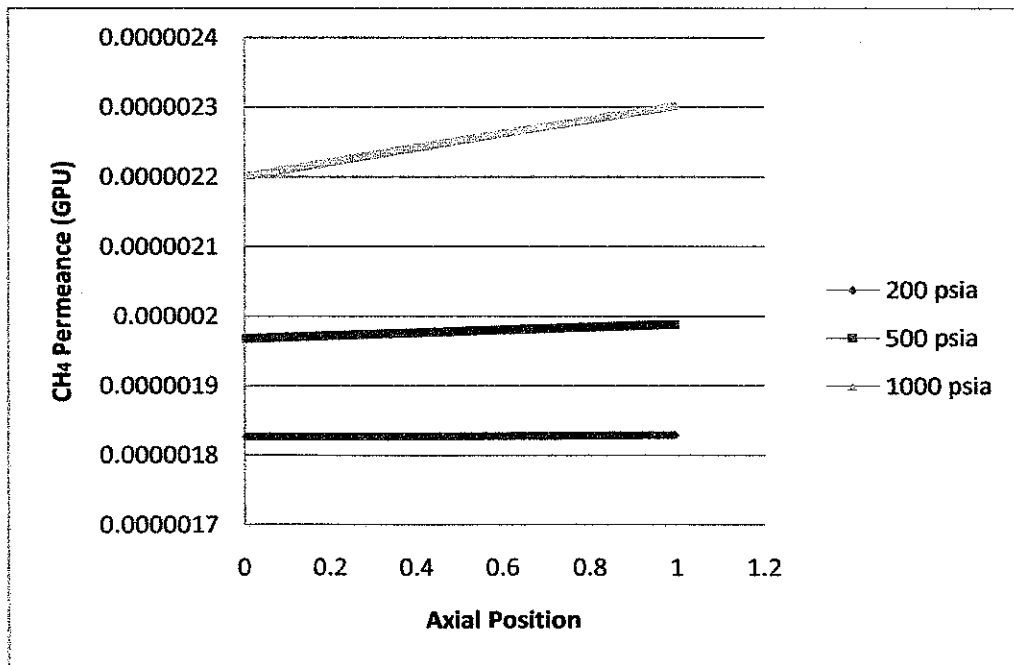Figure A5: Effect of CH₄ concentration towards different feed composition

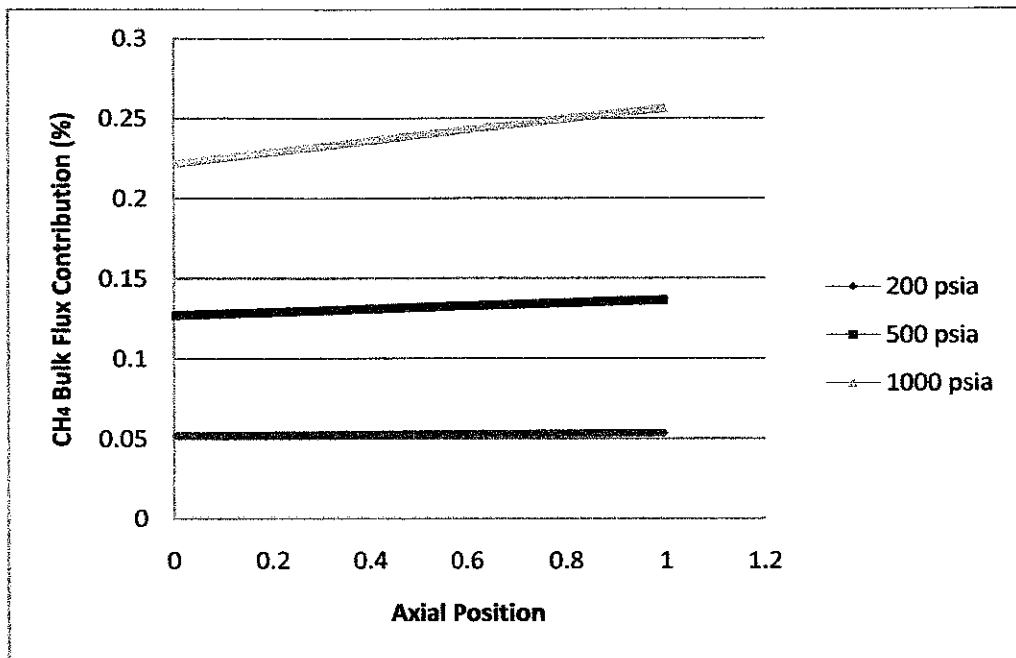Figure A6: Effect of CH₄ permeance towards different feed pressure

Figure A7: Effect of CH4 bulk flux contribution towards different feed pressure